processing protocols, and advanced databases, in comparison with clinical biobanks. One emerging strategy to enhance quality and capacity in research biobanking is to 'repatriate' aspects to pathology.

Design: The British Columbia (BC) BioLibrary model (figure 1) combines: 1) specialized BSp collection units (BCU) embedded within clinical pathology departments with trained personnel, 2) a BSp catalogue of consented research study donor lists, 3) a BSp distribution system in parallel with analysis capacity, and 4) oversight through an interdisciplinary governance structure and molding by public deliberation.

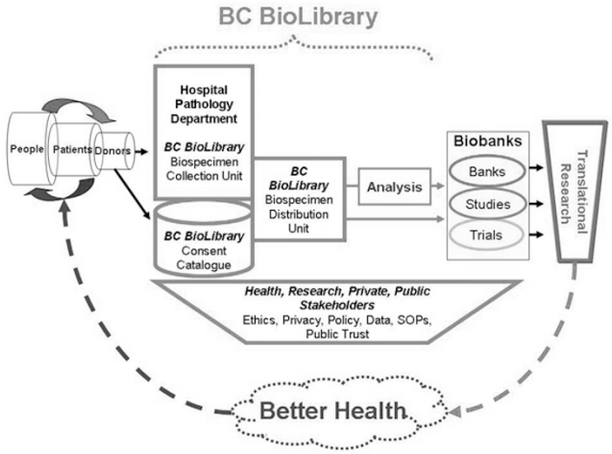

Results: The first BCU has been established and has collected more than 20 BSp. The BC BioLibrary is embraced by leaders in biobanking, pathology, and translational research, from multiple institutions, disease focused research groups and BC funding agencies. This success in engagement and support is driving a pilot phase that will also mold the final design and governance of the model.

Conclusions: The Biolibrary model is designed to maximize the injection of consented, high quality, annotated biospecimens into all forms of biobanks. An opportunity for oversight of biospecimen use, standardization of collection, and equity in distribution to biobanks is created. In the future, this model can promote the harmonization of consent processes and biobanking procedures for processing, storage, and annotation. By creating a common infrastructure, the model reduces competition between biobanks and the tissue providers, offers a transparent process for donors and enhances public trust in biobanking.

1700 Is ER and/or PR Expression Specific Enough To Confirm the Diagnosis of Metastatic Carcinoma of Breast or Gynecological Origin?

S Wei, N Said-Al-Naief, O Hameed. University of Alabama School of Medicine, Birmingham.

Background: Estrogen receptor (ER) and progesterone receptor (PR) are commonly expressed in breast and gynecological carcinomas, and are sometimes used to "confirm" the mammary origin of an adenocarcinoma at a metastatic site, especially when the primary tumor is positive for one or both of these markers. This is despite previous reports that have shown that a variable proportion of non-mammary/non-gynecological adenocarcinomas can also express ER, which would appear to limit their usefulness in this regard. The aim of this study was to systematically evaluate the frequency of ER and PR expression in various non-mammary/non-gynecological adenocarcinomas to further clarify this issue.

Design: Commercially available paraffin-embedded tissue microarrays (TMAs) of malignant tumors of a variety of human organ systems [78 primary lung carcinomas (34 adeno, 33 squamous cell, 1 sarcomatoid, 1 large cell, and 9 small cell), 72 gastric adenocarcinomas, 40 esophageal carcinomas (9 adeno, 29 squamous cell, 1 small cell and 1 sarcomatoid), 78 colonic adenocarcinomas, 20 renal cell carcinomas (clear cell type), and 20 urothelial carcinomas] were immunhistochemically stained for ER (clone 6F11, prediluted, Ventana) and PR (clone 1A6, prediluted, Ventana), with appropriately reactive negative and positive controls. Tumors were scored as positive when any unequivocal nuclear-staining was identified regardless of strength.

Results: Nuclear expression of ER or PR was not detected in any of the primary lung carcinomas, gastric adenocarcinomas, esophageal carcinomas, colonic adenocarcinomas, renal cell carcinomas, or urothelial carcinomas. While ER was not expressed, PR was detected in one case (1/40, 2.5%) of pancreatic ductal adenocarcinomas. Interestingly, PR immunoreactivity was occasionally found in normal stromal cells of bladder regardless of gender.

Conclusions: 1) Although some previous reports suggest otherwise, in the appropriate clinical and histological settings, the lack of ER and PR expression in the tissues evaluated in this study suggest that the addition of ER/PR to a panel of other markers may be particularly helpful in confirming the breast/gynecological origin of a metastatic carcinoma of unknown primary. 2) The lack of nuclear expression of ER/PR does not support these transcription factors having a significant role in tumorigenesis in these organ systems.

1701 Whole Slide Imaging Digital Pathology: A Pilot Study Using Paired Subspecialist Correlations

DC Wilbur, K Madi, RB Colvin, LM Duncan, WC Faquin, JA Ferry, MP Frosch, SL Houser, RL Kradin, GY Lauwers, DN Louis, EJ Mark, M Mino-Kenudson, J Misdraji, GP Nielsen, MB Pitman, A Rahemtullah, AE Rosenberg, RN Smith, JR Stone, RH Tambouret, C-L Wu, RH Young, A Zembowicz, W Klietmann. Massachusetts General Hospital, Boston, MA; University Federal de Rio de Janeiro, Rio de Janeiro, Brazil; Harvard Medical School, Boston, MA; Corista LLC, Concord, MA.

Background: Whole slide imaging technology offers promise for rapid Internet-based telepathology consultations between institutions. Technical issues, pathologist adaptability, and morphologic pitfalls inherent to this process have not been well characterized.

Design: Histopathology slides of diseases from a variety of anatomic sites with reference diagnoses were selected by an outside laboratory. Virtual slides were made using a Zeiss Mirax scanner. Virtual and glass slides were diagnosed independently by 2 subspecialty pathologists appropriate for each anatomic site. Reference diagnoses were compared to virtual and glass slide interpretations, and correlation data was tabulated. Comments on virtual slide technical issues were gathered.

Results: 53 cases were analyzed. There was agreement between virtual, glass, and reference diagnoses in 45 (85%), and between virtual and glass diagnoses in 48 (91%) cases. There were 5 virtual cases (9%) discordant with both reference and glass slide diagnoses. Further review of these cases indicated an incorrect virtual slide interpretation. By anatomic site, concordance rates between virtual and glass slide reviews were: lung - 89% (8/9), liver/GI tract - 82% (9/11), cardiovascular - 100% (5/5), hematopathology - 80% (4/5), thyroid/salivary gland - 100% (6/6), skin - 50% (1/2), kidney - 100% (6/6), prostate - 100% (1/1), gynecologic - 100% (4/4), bone and soft tissue - 100% (3/3), and neuropathology - 100% (1/1). Neoplastic cases showed better correlation (93%) than did cases of non-neoplastic disease (88%). Comments on discordant cases related to virtual slide technical issues such as fine resolution and navigating ability at high magnification.

Conclusions: Overall concordance between virtual and standard slide interpretations was good at 91%. Adjustments in technology, case selection, and further experience to include identification of pitfalls and technology familiarization should improve performance, making digital whole slide review feasible for broader telepathology application.

Ultrastructural

1702 Use of Electron Microscopy in Core Biopsy Diagnosis of Oncocytic Renal Tumors

NA Belsley, MM Johnson, MK Selig, GP Nielsen. Beth Israel Deaconess Hospital, Boston; Massachusetts General Hospital, Boston.

Background: Renal tumor biopsies are being performed more frequently, with the increased detection of small lesions and the use of minimally invasive therapies like radiofrequency ablation (RFA). Distinction between oncocytoma (OC) and chromophobe renal cell carcinoma (CR) on core biopsy is important to guide management. At one of our institutions (MGH), CR is resected or ablated, whereas OC may be clinically followed, with indeterminate lesions treated as CR. Our aim was to evaluate the use of electron microscopy (EM) in distinguishing between OC and CR on needle core biopsies.

Design: The MGH case files were searched for renal core biopsies with a diagnosis of OC, CR or granular cell tumor, indeterminate (GT). Cases in which paraffin blocks were unavailable or in which there was insufficient tissue for EM were excluded. H&E-stained slides as well as any special stains (*i.e.* colloidal iron) or immunohistochemical stains (IC) ordered were reviewed. EM on formalin-fixed, paraffin-embedded tissue was then performed and used as the gold standard to measure the sensitivity and specificity of renal biopsy in differentiating OC from CR.

Results: Fifty-five biopsies of granular cell tumors were identified. After excluding those with unavailable blocks or insufficient tissue for EM, 20 cases remained. Of these, 13 (65%) cases carried a diagnosis of OC, 4 (20%) of CR and 3 (15%) of GT. Diagnosis was aided by colloidal iron in 11 cases, by IC in 2 cases and by EM in 3 cases. By EM, 6 CRs (3 CRs, 1 OC and 2 GTs by initial review) and 14 OCs (1 CR, 12 OCs and 1 GT by initial review) were diagnosed. Ultrastructural detail was variable, but diagnoses were confidently rendered on all cases by two microscopists. The sensitivity and specificity without routine EM (excluding GCT) was 75% and 92%, respectively. Five patients underwent resection, confirming the EM diagnosis, and 3 patients had RFA. No further follow-up was available.

Conclusions: OC and CR can be difficult to differentiate, especially in a limited sample, as their histologic features often merge. Colloidal iron and IC may be of use, but with a clinical branch point of therapy versus follow-up, correct diagnosis is crucial. EM can be useful, even using small, formalin-fixed, paraffin-embedded tissue samples. In this study, one false negative and one false positive were revealed by EM; both were initially managed with RFA. With more certainty in diagnosing granular cell tumors, risk of treatment, cost of follow-up and patient anxiety can be diminished.

1703 Ultrastructural Characterization of Amyloidoma by Scanning and Transmission Electron Microscopy

CA Garcia, SI Gamb, DV Miller. University of Illinois - Peoria, Peoria, IL; Mayo Clinic, Rochester, MN.

Background: Amyloidomas are localized mass-forming deposits of amyloid that occur with or without association with systemic amyloidosis. Amyloidomas may contain AL, AA, senile, dialysis related, or heredofamilial forms of amyloid. Amyloidomas have been well characterized in terms of their histologic, histochemical, and immunohistochemical

characteristics, but there are no detailed reports describing their ultrastructural morphology using scanning electron microscopy (SEM) and transmission electron microscopy (TEM).
Design: The aim of this study was to examine amyloidomas from 2 patients with systemic AL amyloidosis by both SEM and TEM, then compare findings with those accepted for non-amyloidoma amyloid deposition.
Results: Tissues were obtained at autopsy from amyloidomas of the heart in a 58-year-old female and the lung and kidney in a 73-year-old male. Both patients died from complications of primary systemic AL type amyloidosis. Tissues were fixed in glutaraldehyde and processed per routine for SEM and TEM as well as in formalin for paraffin embedding. The amyloidomas showed typical histologic features and appropriate reactions on Congo Red and Alcian Blue staining. TEM demonstrated aggregates of randomly oriented non-branching fibrils showing considerable variability in fibril diameter. Morphometry revealed two subsets of fibrils, one 12-14 nm in average diameter and another averaging 28-30 nm. The larger fibrils showed features of microtubule formation, with apparent lumens evident on cross section. These two groups, as well as the microtubules, were intimately intermixed. In general, the fibrils also tended to adopt a more curvilinear appearance than the typical straight fibers of amyloidosis. Scattered clusters of striated collagen fibers were also present. SEM demonstrated complex 3-dimensional tangles of fibrils, again showing significant variation in width and appearing thicker than typical amyloid fibrils (30-40 nm).
Conclusions: Unlike the amyloid fibrils seen in non-amyloidoma deposits, fibrils within amyloidomas show greater variability in fibril thickness (with diameters approaching 30 nm), microtubule formation, and curvilinear morphology. These findings add to the current ultrastructural and morphologic spectrum of paraprotein deposition disease.

1704 Uterine Tumors Resembling Ovarian Sex Cord Stromal Tumors (UTROSCTs): An Ultrastructural Analysis of 13 Cases

M Gupta, MK Selig, E Oliva, GP Nielsen. DHMC, Lebanon, NH; MGH, Boston, MA.
Background: UTROSCTs are rare tumors that display morphological and immunohistochemical similarities to ovarian sex cord stromal tumors. Their histogenesis is still unclear, as the tumor cells are immunophenotypically diverse and exhibit variable epithelial, sex cord and smooth muscle differentiation. The goals of this study were to analyze the ultrastructural features (EM) of a series of UTROSCTs to ascertain the line/s of differentiation and to correlate these findings with their immunohistochemical profile (IHC).
Design: Thirteen UTROSCTs were retrieved from archival material. All available HE slides were reviewed to confirm the diagnosis. Representative areas were chosen from preexisting paraffin blocks. The ultrastructural findings were correlated with IHC results from a previous analysis in 10/13 cases.
Results: The tumors frequently had an organoid, nested or cord-like arrangement (8), 2 of them showing lumen formation with associated microvilli in one. The nuclei showed irregular indentations in 8 tumors. Intermediate filaments were seen in 13/13 UTROSCTs and in 5 they formed prominent paranuclear aggregates imparting a rhabdoid morphology; cell junctions were found in 9/13, desmosomes in 1 and definite tonofilaments in 2. Basal lamina was identified in 1 case. No dense bodies, subplasmalemmal densities or pinocytic vesicles were seen. Seven tumors showed cytoplasmic lipid droplets (prominent in 3). EM evidence of epithelial differentiation was present in 3 cases (1 with desmosomes, 2 with tonofilaments; IHC positive for keratin or EMA). Prominent lipid content by EM was seen in 3 UTROSCTs and correlated with positive IHC for sex cord markers in 2/3. Presence or absence of abundant paranuclear intermediate filaments did not correlate with smooth muscle IHC markers.
Conclusions: Our findings indicate that UTROSCTs are polyphenotypic neoplasms at the ultrastructural level and show evidence of variable sex cord like and focal epithelial differentiation. These findings overlap with those described in sex-cord stromal tumors of the ovary. In contrast to previous studies, we did not find evidence of smooth muscle differentiation in any of the cases although preservation of the tissue was suboptimal. These findings suggest that expression of smooth muscle markers by IHC may be non-specific as it occurs in sex cord stromal tumors of the ovary. UTROSCTs may result from divergent differentiation in endometrial stromal tumors or represent a distinct group with variable degree of sex cord-like differentiation.

1705 Calcifying Fibrous (Pseudo)Tumor: Review of Histopathologic, Immunocytochemical and Ultrastructrual Features

J Hicks, G Mierau. Texas Children's Hospital, Baylor College of Medicine, Houston, TX; The Children's Hospital, Denver, CO.
Background: Calcifying fibrous tumor (also known as calcifying fibrous pseudotumor) is a rare tumor that afflicts children, adolescents and young adults. In the past, it has been considered to be the end-stage of inflammatory myofibroblastic tumor; however, certain characteristics distinguish it as a separate entity. Most pediatric tumors involve soft tissues, although visceral tumors are known to occur. There have been rare reports of familial cases.
Design: The study population consisted of 5 children (age range 1-5.5 years, 3M:2F) with tumors involving lumbar spine, axilla, chest, head and neck, and paratesticular area. Tissue was available for routine, immunocytochemical and electron microscopic examination. Immunocytochemical (vimentin, CD34, factor XIIIa, ALK-1, S100 protein, SMA, MSA) and ultrastructural evaluation was performed. Tissue was submitted for cytogenetic study with 3 cases. Localized recurrence occurred in 2 children.
Results: The tumors were composed of densely collagenized stroma with infrequent fibroblasts with a moderate amount of cytoplasm. Stromal calcifications of both psammatous and dystrophic types were embedded in the collagen with no evidence of osteoblastic cells. Occasional lymphoid aggregates and scattered lymphoplasmacytic cells were noted. Immunocytochemistry demonstrated diffuse vimentin and moderate factor XIIIa cytoplasmic expression. Tumor cells were negative for ALK-1, CD34, SMA, MSA and S100 protein. Electron microscopy revealed abundant collagen with occasional fibroblasts, characterized by dilated rough endoplasmic reticulum. Fibroblasts and collagenous matrix were in close proximity to calcified tissue. There were relatively frequent mast cells. Cytogenetics in 3 cases showed no ALK rearrangement or chromosomal abnormalities.
Conclusions: Calcifying fibrous tumor failed to demonstrate ALK-1, SMA, MSA, myofibroblastic ultrastructural features, or clonal ALK-1 gene rearrangements, characteristic of infammatory myofibroblastic tumors. These features are important in distinguishing these tumors from one another. Relatively frequent mast cells within calcifying fibrous tumor raises the possiblity of mast cell influence on tumorigenesis. In certain fibroblastic proliferations with calcifications (fibrodysplasia ossificans progressiva), mast cells have been implicated and are increased by up to 150-fold over normal fibroconnective tissue. Agents directed against mast cells have been suggested as potential novel therapy in certain fibroblastic tumors.

1706 Infantile Rhabdomyofibrosarcoma: Variant of Congenital Infantile Fibrosarcoma

J Hicks, M Lovell, G Mierau. Texas Children's Hospital, Baylor College of Medicine, Houston; The Children's Hospital, Denver.
Background: Congenital infantile fibrosarcoma (CIF) is a well-recognized, rare fibrosarcomatous tumor arising *in utero* or in the 1st year of life. CIF is an asymptomatic, rapidly growing tumor involving distal extremities with a favorable prognosis. CIF has a nonrandom translocation [t(12;15)-ETV6-NTRK3] detected by cytogenetics, FISH and RT-PCR (isolated reference/research labs). Infantile rhabdomyofibrosarcoma (IRF) shares certain features with CIF, but has infrequent to rare spindled rhabdomyofibrosarcoma cells and frequent fibrosarcoma cells. IRF tends to behave in a more aggresive manner.
Design: Study population consisted of 10 infants (age range 3d to 10mos) with CIF and 4 infants (age range 10d to 8ms) with IRF. Tumors were all located in distal extremities. Tissue was available for routine, immunocytochemical (vimentin, MSA, myogenin, desmin) and ultrastructural studies. Cytogenetics and/or FISH (ETV6/TEL breakapart) study results were available in a limited number of cases (6 CIFs; 3 IRF).
Results: CIFs and IRFs were highly cellular tumors with closely packed, plump spindled and ovoid cells with a high nuclear to cytoplasm ratio and frequent mitotic figures. Infiltration of soft tissue and skeletal muscle was noted in several cases. Strap cells and classic rhabdomyoblasts were not present. Immunocytochemistry demonstrated diffuse vimentin and focal MSA staining for CIFs and IRFs. Rare IRF ovoid to spindled tumor cells expressed desmin, myogenin and MSA. Electron microscopy with both CIFs and IRFs revealed fibrosarcomatous features. Stroma contained fine fibrillary material, infrequent collagen and dense granular "amorphous" material (characteristic for CIF). With IRFs, rare spindled fibrosarcoma-like cells possessed myofilaments, rudimentary z-band material and a dense surface glycocalyx. Cytogenetic and FISH found that most CIFs (5/6) and all IRFs (3/3) had rearrangement of ETV6/TEL consistent with t(12;15) translocation.
Conclusions: Infantile rhabomyofibrosarcoma has been considered a distinct entity, separate from congenital infantile fibrosarcoma. IRF and CIF share certain immunocytochemical (vimentin, focal MSA in fibrosarcomatous cells) and ultrastructural features (fibrosarcomatous cells, fine fibrillary material, infrequent collagen, granular amorphous material). IRF is distinguished by rare rhabdomyofibrosarcomatous cells with myogenic features (desmin, myogenin, MSA, myofilaments, z-bands). IRFs should be classified as a CIF variant, due to sharing a nonrandom rearrangement (ETV6-NTRK3).

1707 Tissue Distribution of Treponema Pallidum in Primary and Secondary Syphylis: An Ultrastructural Study

N Juanpere, G Martin-Ezquerra, A Fernandez-Casado, L Magan, MA Garcia, C Barranco, S Serrano, RM Pujol, J Lloreta. Hospital del Mar, Barcelona, Spain; UAB, Barcelona, Spain; Universitat Pompeu Fabra, Barcelona, Spain.
Background: In recent years, an increase in the prevalence of syphilis has been observed. Identification of the causative organism is nowadays more efficient with the advent of highly specific and sensitive antibodies. There are limited reports on the ultrastructure of skin lesions caused by Treponema pallidum. The aim of the present study has been to investigate the tissue distribution of the microorganisms in both the primary infection and the secondary lesions.
Design: One case each of primary syphilitic chancre and secondary syphilis were included in this study. Paraffin sections of both cases were stained with anti-treponema antibody (BioCare Medical, Concord, CA). Tissue for electron microscopy was retrieved from the paraffin bloc with a tissue microarray needle (0.1 mm). The samples were deparaffinized, fixed in osmium tetroxide and embedded in resin. Thin sections were examined under a CM100 electron microscope.
Results: Histologically, both lesions showed characteristic features, with more prominent epidermal changes in the primary chancre, and a more diffuse, perivascular infiltrate in the secondary lesion. Immunohistochemistry revealed abundant perivascular Treponema clusters in the chancre, and obvious intraepidermal microorganisms in the secondary lesion. Ultrastructurally, spirochaetes were located almost exclusively in the blood vessel walls in the chancre. In secondary syphilis, they were paradoxically more abundant between epidermal keratinocytes and adnexal epithelial cells, although some could also be found in the vessel walls, amidst smooth muscle cells. In all cases, they adjusted into the intercellular spaces between adjacent cells. In some sections of the secondary lesion, deep invaginations of the keratinocytes seemed to partially engulf the spirochaetae, but no intracellular organisms were found.

Conclusions: Ultrastructural and immunohistochemical examination of primary and secondary syphilis lesions show a paradoxical distribution of the causative microorganisms, as they tend to be more abundant in the blood vessels of primary and in the epidermis of secondary lesions. The close relationship with the adjacent smooth muscle and epithelial cells suggests that pathogenic mechanisms similar to intestinal spirochaetosis or Helicobacter pylori infection may be involved in luetic lesions.

1708 Acinar Cell Cystadenoma of the Pancreas: Role of Electron Microscopy

AJ Saenz, MK Selig, GP Nielsen, V Deshpande. James Homer Wright Pathology Laboratories, Massachusetts General Hospital, Boston, MA.

Background: Acinar cell cystadenoma of the pancreas (ACA) is a rare benign cystic neoplasm of the pancreas characterized by a cyst lining showing acinar cell differentiation. This study investigates the role of ultrastructural evaluation in the diagnosis of ACA.

Design: Benign unclassified pancreatic cysts were retrieved from the files of the Massachusetts General Hospital. Electron microscopy (EM) was performed on tissue retrieved from paraffin. Immunohistochemistry was performed on selected cases.

Results: We identified six benign pancreatic cysts that could not be definitively classified with the available evidence. The patients were all women with an age range of 31 to 63 (mean 44.5) years. All of the neoplasms were cystic radiographically and grossly with a size range of 0.3 to 7.5 cm (mean 3.5 cm). None of the cysts communicated with the pancreatic ductal system. Histopathologically, the cysts were lined by a single layer of non-specific cuboidal epithelium. On EM, variably sized electron dense zymogen granules were identified in one case (case 1) and stacked rough endoplasmic reticulum was identified in two cases (case 1 & 2). Case 1 is a 24 year-old female with a multilocular cystic lesion in the head of the pancreas; Case 2 is a 31 year-old female with a multilocular cystic lesion in the tail of the pancreas. On immunohistochemistry, the lining epithelium of these two cases were positive for trypsin, cytokeratin, and negative for chromogranin and synaptophysin. The other four cases lacked ultrastructural evidence of acinar cell differentiation.

Conclusions: Ultrastructural evaluation uncovered evidence of acinar cell differentiation in two cases which was corroborated by immunohistochemistry. This study suggests that ultrastructural evaluation could assist in the definitive classification of otherwise ‘unclassified’ benign pancreatic cysts.